# Supplemental Figure 1

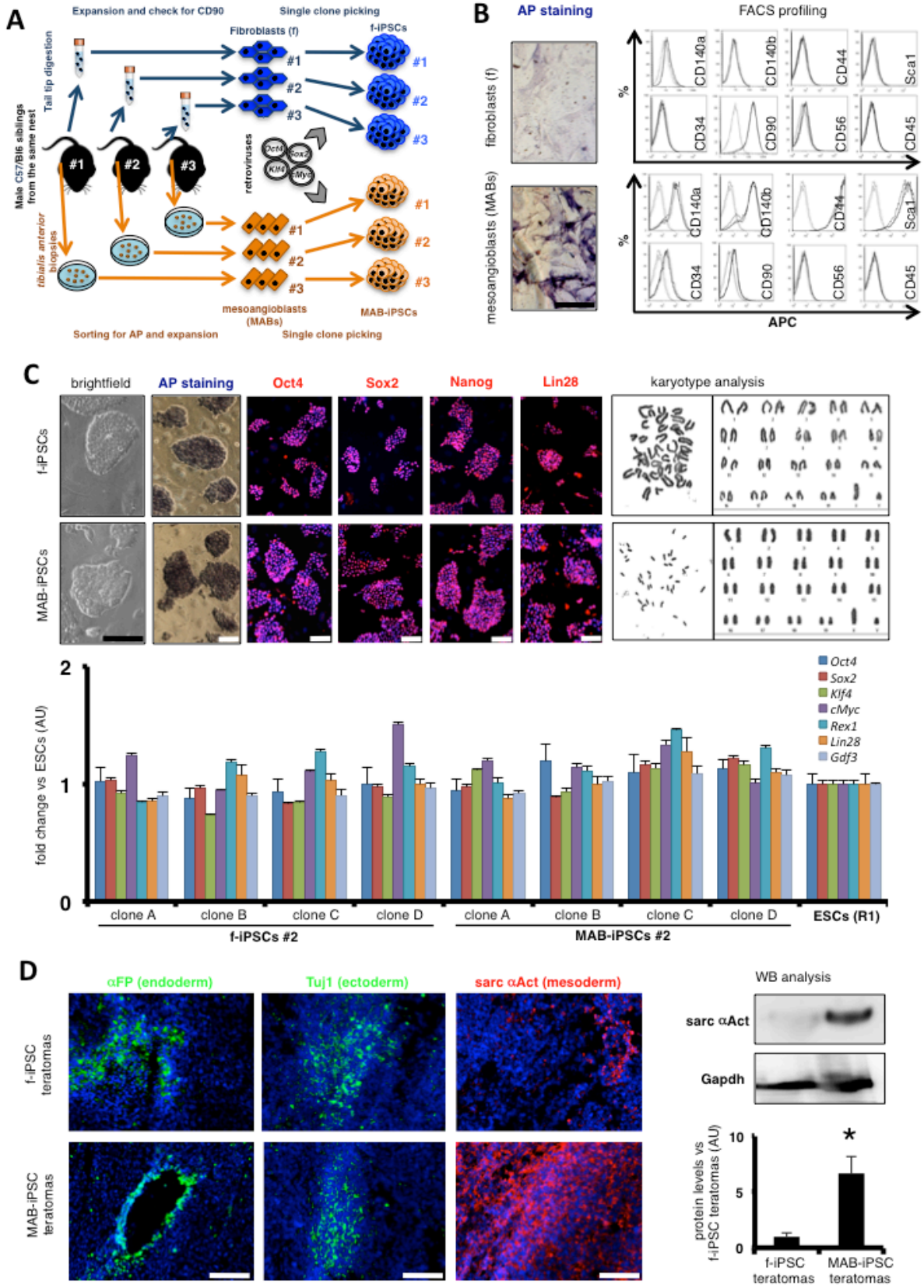

**Supplemental Figure 1. Validation of syngenic/isogenic system for myogenic memory assessment.** (**A**) Summary of experimental plan and procedures used for the murine iPSC study in syngenic/isogenic conditions. Reprogramming factors were of murine origin and transduced by means of retroviral vectors. (**B**) After FACS isolation, murine MAB lines resulted positive to alkaline phosphatase (AP) staining, unlike isogenic fibroblasts. Cytometry profiling at passage 3 showed that fibroblasts were $CD90^+$ and slightly $CD140a^+$, whereas MABs resulted $CD140a^+/CD140b^+/CD44^+/Sca1^+$, partially $CD34^+/CD90^+$, and $CD56^-/CD45^-$ (pan-isotype controls, light grey; stained samples, dark grey; depicted are data from #1/2/3 lines for each cell type). (**C**) Isogenic f- and MAB-iPSCs showed comparable morphology and expression pattern of pluripotency markers. G-banded chromosome spreads and related karyograms showed ≥70% euploidy and absence of specific aneuploidies in clones of murine f- and MAB-iPSCs at passage 3 (n≥10 spreads per iPSC clone). qPCR-based quantification indicated comparable levels of pluripotency marker expression among f- or MAB-iPSC clones at passage 3, when compared to R1 ESCs. AU, arbitrary units; error bars, standard deviation. Depicted in C are all data from f- and MAB-iPSCs from individual #2, results from individuals #1/3 are analogous. (**D**) Teratomas were obtained at 4-6 weeks after subcutaneous injection of isogenic f- and MAB-iPSCs in *Rag2-null/γc-null* immunodeficient mice and displayed endodermal (alpha-fetoprotein$^+$, $\alpha FP^+$), ectodermal (beta-III tubulin$^+$, Tuj1$^+$), and mesodermal (sarcomeric alpha-actinin$^+$, sarc aAct$^+$) derivatives, albeit the immature muscle patches were dramatically more present in MAB-iPSC-derived teratomas, as also confirmed by WB and Gapdh-normalized densitometry analysis (*, $P<0.05$, n=3/iPSC type, Mann Whitney U test; AU, arbitrary units; error bars, standard deviation. Scale bars, approximately 100μm.

## Supplemental Figure 2

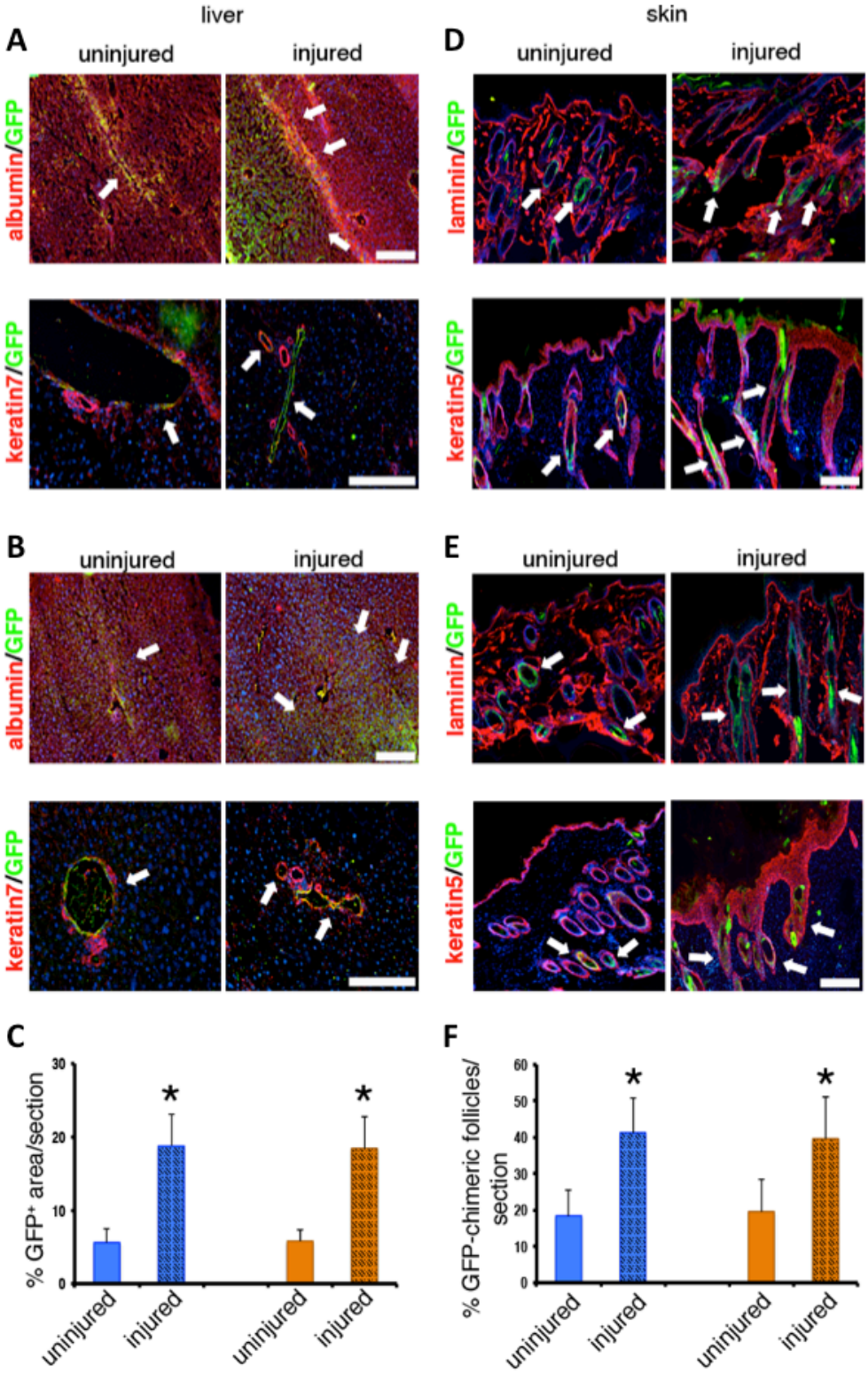

**Supplemental Figure 2. Similar contribution of f- and MAB-iPSCs to endoderm and ectoderm derivatives in chimeric adult mice.** $GFP^+$ f- and MAB-iPSCs contributed to a comparable extent to hepatocytes ($albumin^+$) and bile duct cells ($keratin7^+$) in uninjured (right/median) and regenerated liver lobes (left) (A-C), and to inner/outer root sheets of hair follicles in uninjured and wound-injured skin sites (D-F) of adult chimeric mice at 4 weeks post-injuries. n=4mice/iPSC type; *, $P<0.05$ vs uninj f-iPSC mice; **, $P<0.05$ vs inj f-iPSC mice; Kruskal-Wallis and Mann Whitney U test. Error bars, standard deviation; scale bars, approximately 100μm.

## Supplemental Figure 3

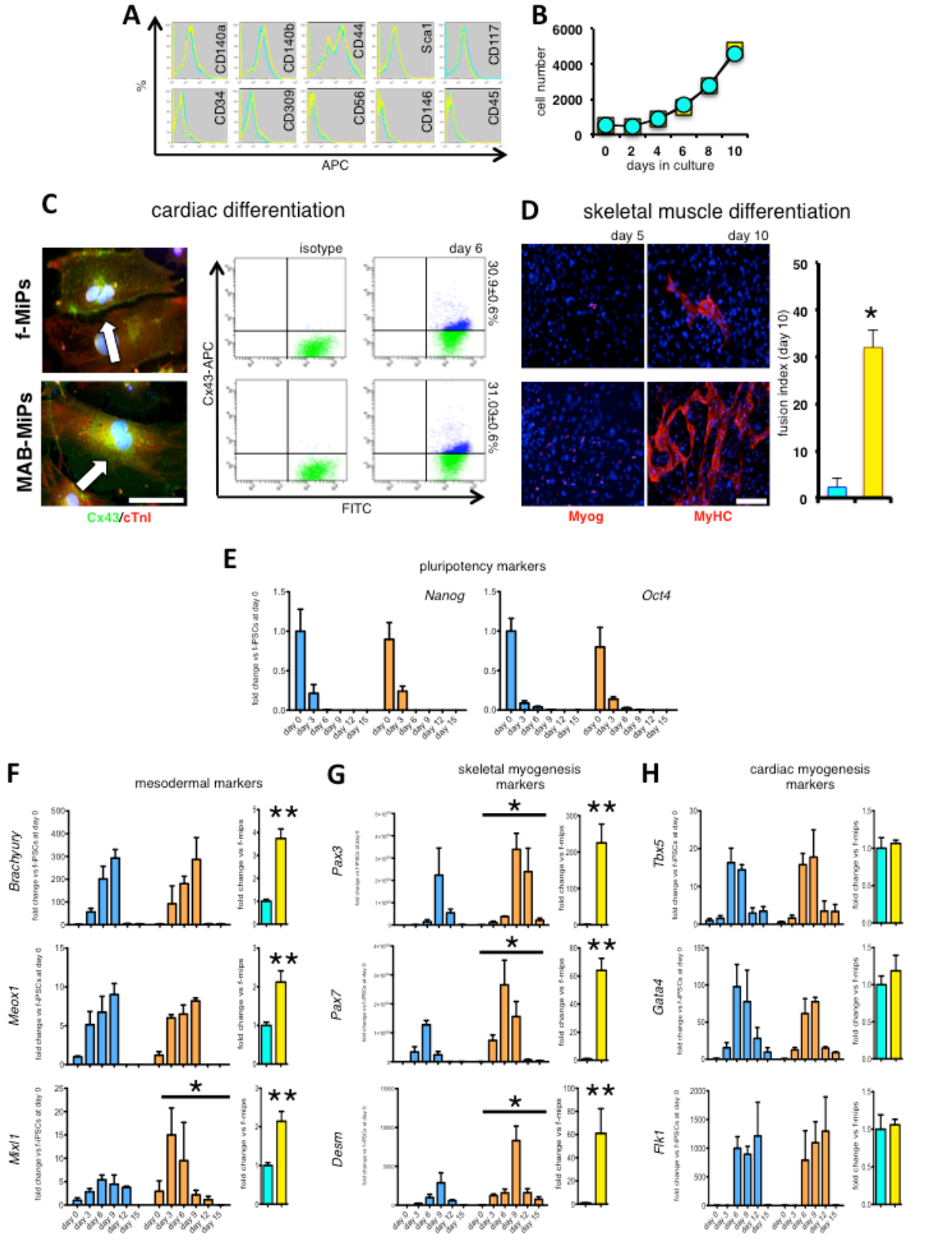

**Supplemental Figure 3. Myogenic memory is durable in iPSC-derived progenitors and is traceable in gene expression pattern over time.** (**A**) Murine f- and MAB-MiPs resulted $CD140a^+/CD140b^+/CD44^+/Sca1^+/CD117^+$, partially $CD34^+/CD309^+$, and $CD56^-/CD146^-/CD45^-$ at cytometry-based profiling at passage 1 (pan-isotype controls, dotted lines; stained samples, full lines; depicted are data from f- (yellow) and MAB-MiPs (light blue)). Once in culture under proliferative conditions, f- and MAB-MiPs displayed comparable growth curves (**B**). (**C**) *In vitro* MiP differentiation to cardiomyocyte-like cells displayed comparable rates of $cTnI^+/Cx43^+$ bi-nucleated cells. (**D**) After transient transfection of f- and MAB-MiPs with *Pax3-Pax7* overexpressing plasmids and subsequent serum starvation, MAB-MiPs presented a higher number of $Myogenin^+$ ($Myog^+$) nuclei at day 5, and of $MyHC^+$ myotubes at day 10, as compared to syngenic f-MiPs, as also quantified by fusion index analysis; *, $P<0.05$, n=4/MiP type; Mann-Whitney U test. Scale bars, approximately 100μm. (**E**) Applying the differentiation conditions used to differentiate iPSCs towards MiPs, qPCR analysis over time showed a progressive decline of pluripotency marker expression (*Nanog, Oct4*) in both f- and MAB-iPSCs, with no significant difference (n=3/iPSC type; 2way ANOVA test). (**F**) Mesodermal marker expression (*Brachyury, Meox1* and *Mixl1*) appeared peaking at day 9 in both f- and MAB-iPSCs. *Brachyury* and *Meox1* trends were not significantly different, whereas *Mixl1* trend over time in MAB-iPSCs was significantly different from f-iPSCs (*, $P<0.05$ for cells/stages; n=3/iPSC type; 2way ANOVA test). Interestingly, when comparing sorted f- and MAB-MiPs, all three markers resulted slightly but significantly upregulated in MAB-MiPs, as compared to f-MiPs (**, $P<0.05$; n=3/MiP type; unpaired t-test). (**G**) Expression trends of skeletal muscle markers (*Pax3, Pax7* and *Desmin*) appeared significantly different between differentiating f- and MAB-iPSCs (*, $P<0.05$ for cells/stages; n=3/iPSC type; 2way ANOVA test). Consistently, when comparing sorted f- and MAB-MiPs, all three markers resulted highly upregulated in MAB-MiPs, as compared to f-MiPs (**, $P<0.05$; n=3/MiP type; unpaired t-test). (**H**) Differently from the skeletal myogenic markers, expression trends of cardiomyogenic markers (*Tbx5, Gata4* and *Flk1*) did not show significant differences between differentiating f- and MAB-iPSCs (n=3/iPSC type; 2way ANOVA test), or between sorted f- and MAB-MiPs (n=3/MiP type; unpaired t-test). AU, arbitrary units; error bars, standard deviation.

## Supplemental Figure 4

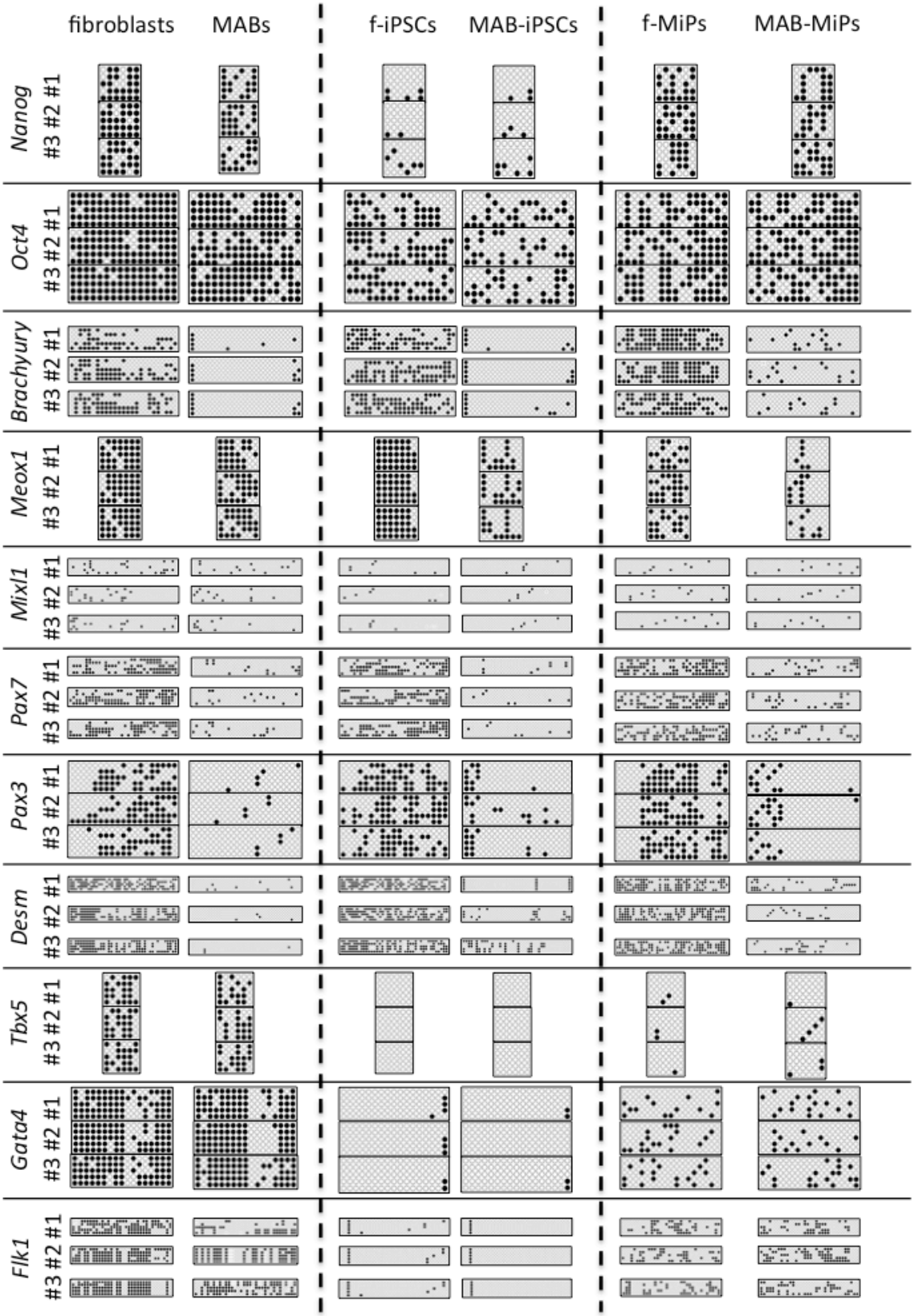

**Supplemental Figure 4 – CpG methylation data, related to analyses presented in Figure 4 and Supplemental Figures 5-6.** Representative CpG methylation data are depicted as dots, each representing a CpG in 5'->3' orientation. White dots depict non-methylated CpG, while black dots depict methylated CpGs. Each dot row represents a CpG island sequence read. Reported in this visual table are 5 reads per cell clone per cell type, each cell clone isolated from a different donor (#1, #2, #3).

## Supplemental Figure 5

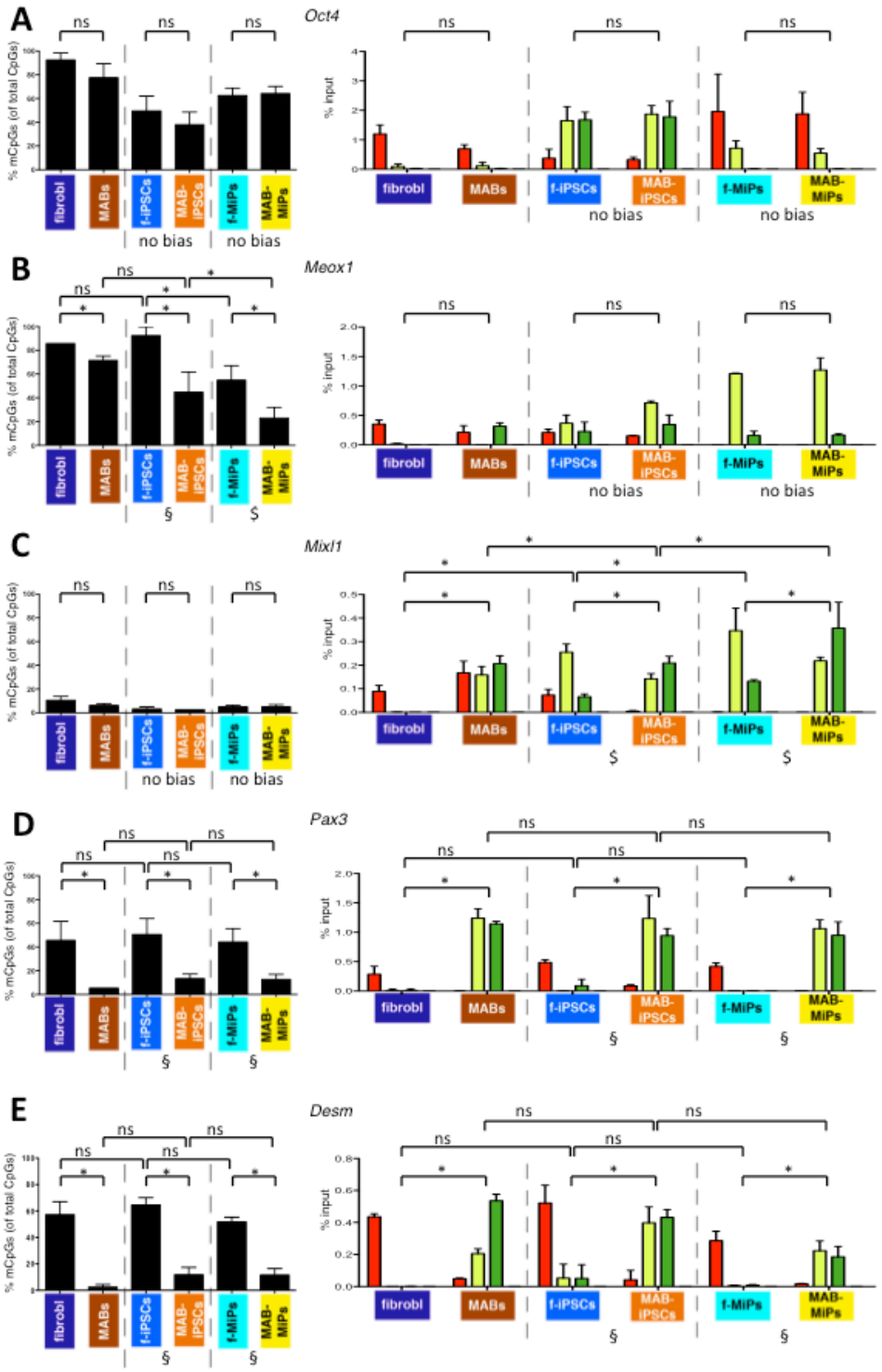

**Supplemental Figure 5. Complementary data of DNA methylation and histone mark enrichment.** (**A**) the pluripotency marker *Oct4* presented stage-specific changes in epigenetic cues, with no progeny-related bias (Q1=ns). (**B-C**) The mesodermal markers *Meox1* and *Mixl1* presented a complex pattern of epigenetic biases. Meox1 showed progeny-related biases only in DNA methylation, as inherited at iPSC stage (§) and as remodeled at MiP stage ($). Conversely, Mixl1 presented remodeled biases ($) at both stages only in histone mark enrichment. (**D-E**) The skeletal myogenesis markers *Pax3* and *Desm* presented inherited biases in both DNA methylation and histone marks at both iPSC (§) and MiP (§) stages. MAB-derived cells showed a durable bias in lower methylation and permissive/activating histone marks. *, $P<0.05$, n=3/cell pool; for DNA methylation analysis, 1way ANOVA test with Bonferroni multi-comparison; for histone mark analysis, 2way ANOVA test with Bonferroni mutli-comparison. All analyses included data from isogenic clones from three syngenic individuals.

## Supplemental Figure 6

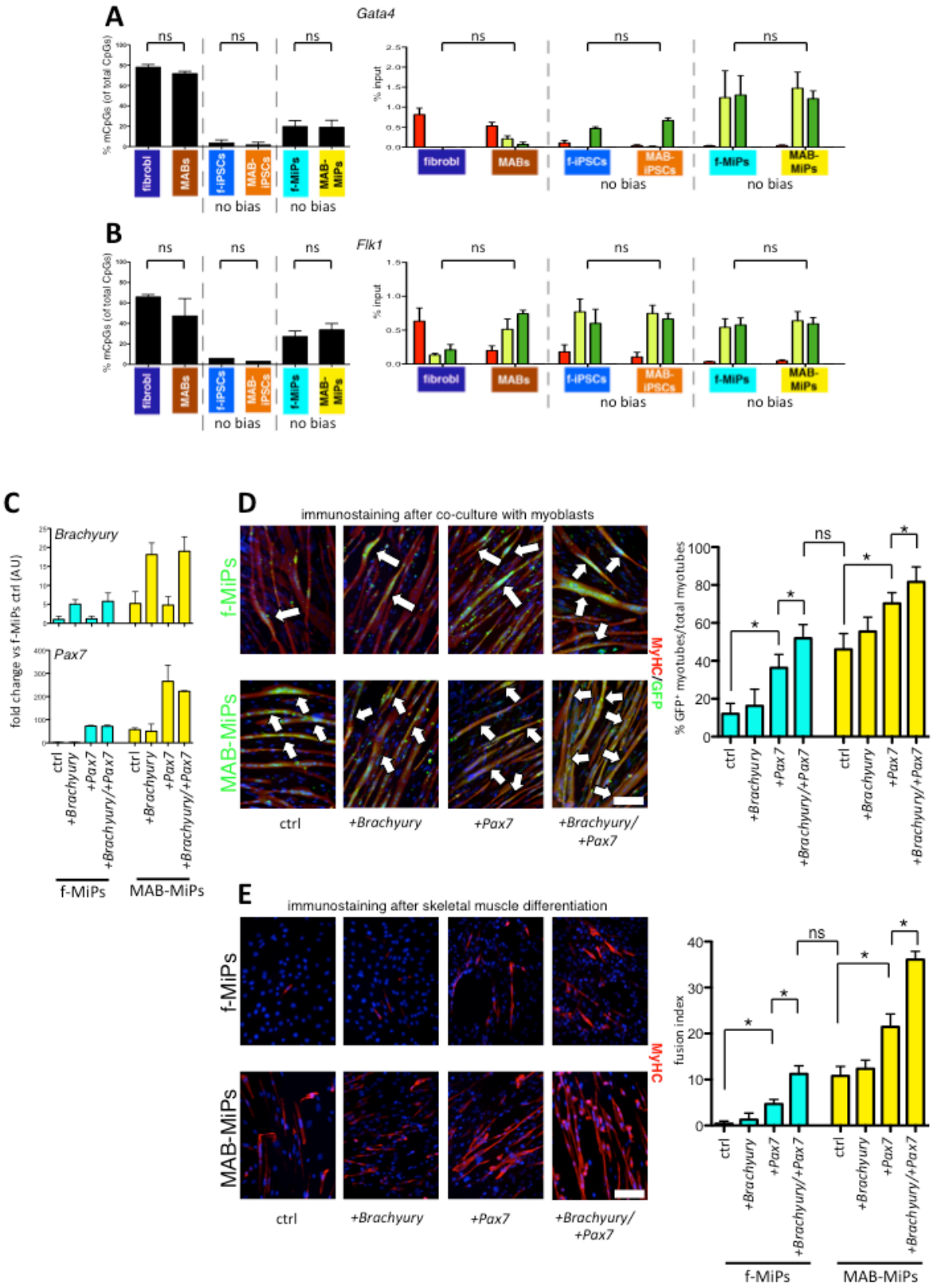

**Supplemental Figure 6. Complementary data of DNA methylation and histone mark enrichment, and effects of pulse of Brachyury/Pax7 on MiP myogenic propensity.**
(**A-B**) The cardiac myogenesis markers *Gata4* and *Flk1* presented stage-specific shifts in methylation and histone marks, with no significant progeny-related bias (Q1=ns). Both MiP types presented low methylation levels and enrichment in H3K27ac. *, P<0.05, n=3/cell pool; for DNA methylation analysis, 1way ANOVA test with Bonferroni multi-comparison; for histone mark analysis, 2way ANOVA test with Bonferroni mutli-comparison. All analyses included data from isogenic clones from three syngenic individuals. (**C**) Transient pulse of Brachyury and Pax7 in f-MiPs induced upregulation levels comparable to control (ctrl) MAB-MiPs at 48 hours post-transfection. Data are depicted as fold change vs ctrl f-MiPs; AU, arbitrary units; error bars, standard deviation. (**D-E**) Combined pulse of *Brachyury* and *Pax7* induced levels of skeletal muscle differentiation in transfected f-MiPs comparable to ctrl MAB-MiPs, as indicated by increase in $GFP^+$ myotube rate in co-culture with myoblasts (**D**, arrows) and in myotube production (quantitated as fusion index, i.e. % of nuclei in $MyHC^+$ myocytes) after skeletal muscle differentiation (**E**). *, P<0.05; n=3/transfection condition; 1way ANOVA with Bonferroni multi-comparison; error bars, standard deviation.

## Supplemental Figure 7

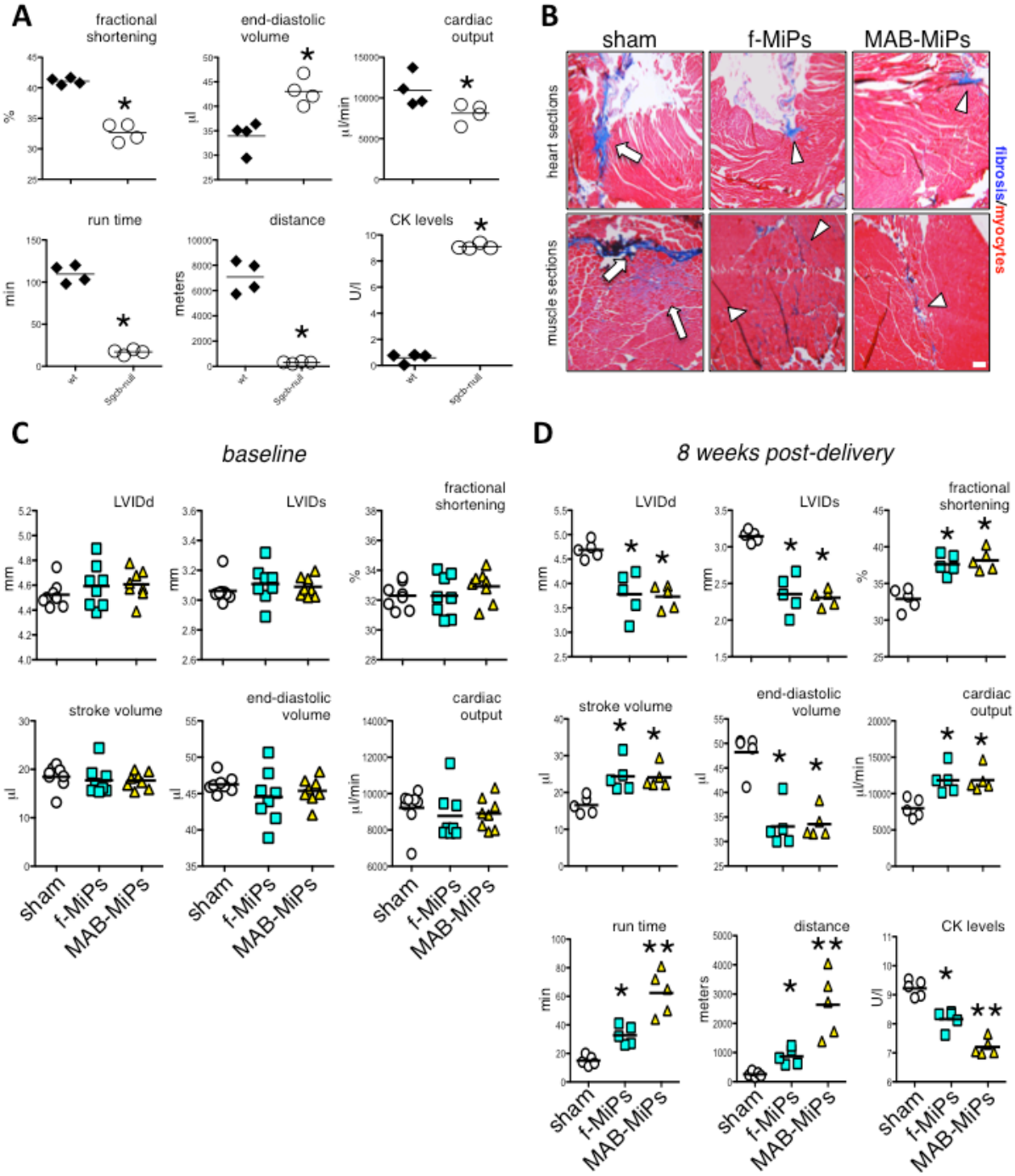

**Supplemental Figure 7. Complementary functional and histologic analyses of murine MiP-driven regeneration.** (**A** upper row) Validation of the dystrophic cardiomyopathy by means of 3D echocardiography. *Sgcb-null* mice showed significant decrease in fractional shortening, increase in ventricular volume and reduced cardiac output, when compared to wt controls (*, P<0.05; n=4/group; Mann-Whitney U test). (**A**, lower row) Validation of impaired mobility and creatine kinase release in the serum. *Sgcb-null* mice performed significantly worse at the treadmill and presented higher serum CK levels, when compared to wt controls (*, P<0.05; n=4/group; Mann-Whitney U test). Each data point refers to one animal, bars depict average values. (**B**) As shown by Masson's trichromic staining at 4 and 8 weeks post-injection, fibrotic scars and/or infiltrations (arrowheads) were comparably reduced in f- and MAB-MiP-treated hearts as compared to sham (upper panels), whereas they appeared consistently more reduced in MAB-MiP- than in f-MiP-treated *quadriceps* muscles. N=8/group; scale bar, approximately 100μm. (**C**) 3D echocardiography analyses at baseline show no significant differences among randomly-distributed mice cohorts; n=8mice/group, Kruskal-Wallis and Mann-Whitney tests. **(D**) According to functional assessment at 8 weeks post-injection, MiP-induced beneficial effects on cardiac functionality appeared durable and comparable between f- and MAB-MiPs. Also, treadmill assay at 8 weeks post-injection evidenced a similar situation to 4 weeks post-injection, i.e. f-MiP injection induced amelioration of the hindlimb mobility, yet this effect was significantly more pronounced in MAB-MiP-injected mice. In addition, luminometric analysis of serum CK levels indicated a significant downregulation in MiP-treated mice and, similarly to results at 4 weeks post-injection, MAB-MiP-injected mice showed significantly decreased levels when compared to f-MiP-treated mice. N=5mice/group; *, P<0.05 vs sham; **, P<0.05 vs sham and f-MiPs; Kruskal-Wallis and Mann-Whitney tests. Each data point refers to one animal, bars depict average values.

## Supplemental Figure 8

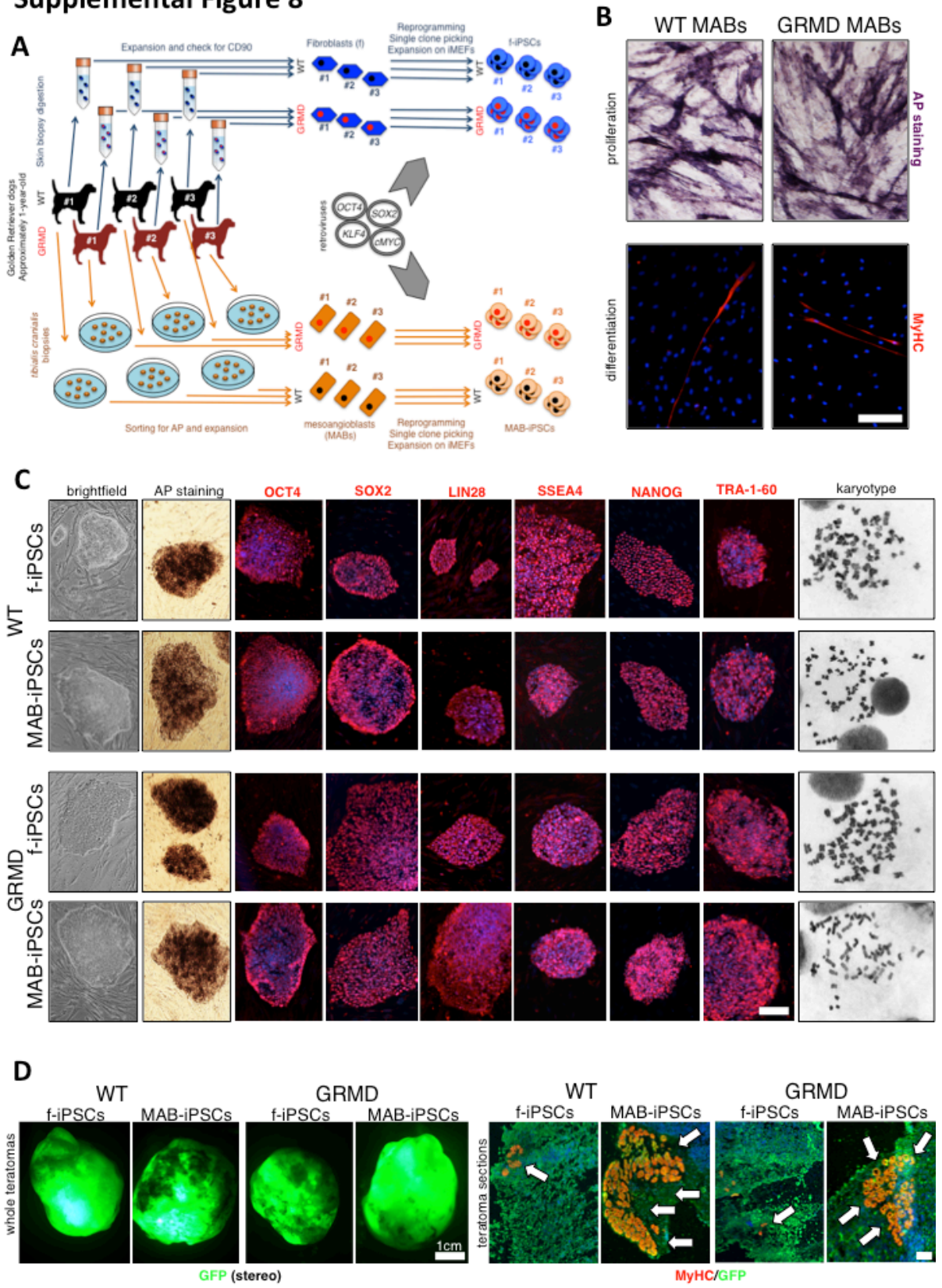

**Supplemental Figure 8. Myogenic memory in isogenic canine iPSC system.** (**A**) Summary of experimental plan and procedures used for the canine iPSC study in isogenic conditions. Reprogramming factors were of human origin and transduced by means of retroviral vectors. (**B**) Once sorted for AP and expanded on collagen, WT and GRMD primary MAB populations appeared homogeneous for AP expression and, under serum starvation, spontaneously differentiated into occasional $MyHC^+$ myotubes, consistently with previous reports. (**C**) After picking and stabilization on iMEFs, canine iPSC clones at passage 3 showed hESC-like morphology and resulted homogeneously positive to AP, OCT4, SOX2, LIN28, and SSEA4 staining. In addition, chromosome spread counts indicated that all screened clones resulted euploid (78 chromosomes). (**D**) $GFP^+$ WT and GRMD iPSCs produced teratomas in analogous conditions to murine iPSCs. However, despite the presence of derivatives from all three germ layers (data not shown), MAB-iPSCs (both WT and GRMD) consistently produced more and larger immature muscle patches as compared to isogenic f-iPSC-teratomas; n=3/iPSC type.

## Supplemental Figure 9

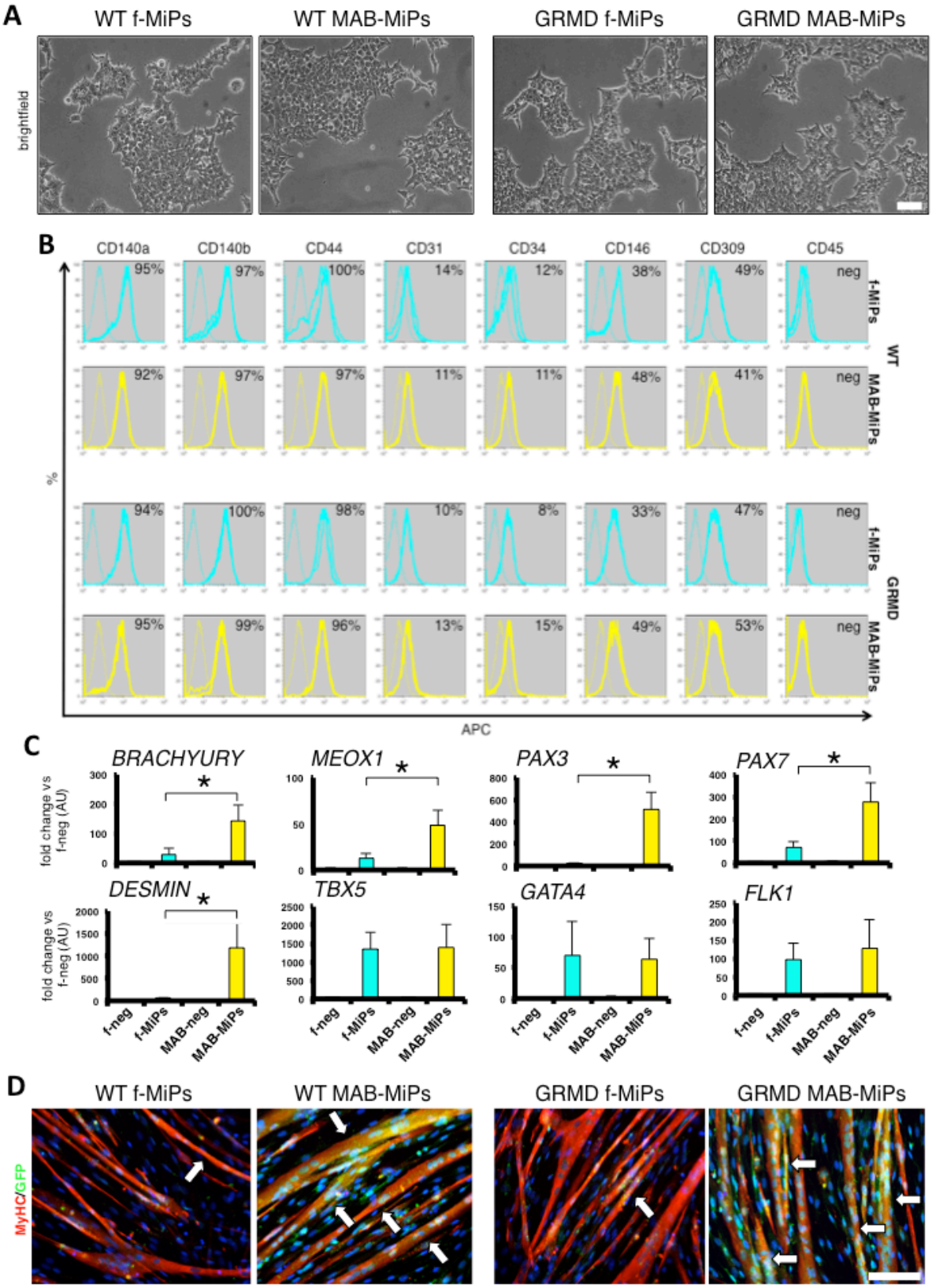

**Supplemental Figure 9. Canine MiP isolation and characterization.** (**A**) Morphology of canine MiPs under proliferative conditions is similar to that of murine MiPs. (**B**) Regardless of genotype or type, canine MiPs appeared homogeneously $CD140a^+/CD140b^+/CD44^+/CD45^-$, and partially $CD31^+/CD34^+/CD146^+/CD309^+$. Pan-isotype controls, dotted line; stained samples, thick lines; depicted are data from #1/2/3 lines for each cell type; quantifications (%) of reported cytometer data are reported as average values. (**C**) qPCR analyses showed that markers of mesodermal commitment, skeletal and cardiac myogenesis were upregulated in WT f- and MAB-MiPs. Interestingly, similarly to the results obtained in murine MiPs, *BRACHYURY*, *MEOX1*, *PAX3, PAX7* and *DESMIN* appeared upregulated in MAB-MiPs, when compared to f-MiPs, whereas the cardiomyogenic markers did not show significant biases in expression. In addition, GRMD MiPs showed similar patterns in gene expression (data not shown). *, $P<0.05$; n=3/cell pool; unpaired t-test. AU, arbitrary units; error bars, standard deviation. (**D**) When compared to isogenic f-MiP controls, both WT and GRMD $GFP^+$ MAB-MiPs produced a higher number of GFP-chimeric myotubes (arrows) in co-culture with myoblasts; n=4/MiP type. Scale bar, approximately 100μm.

## Supplemental Figure 10

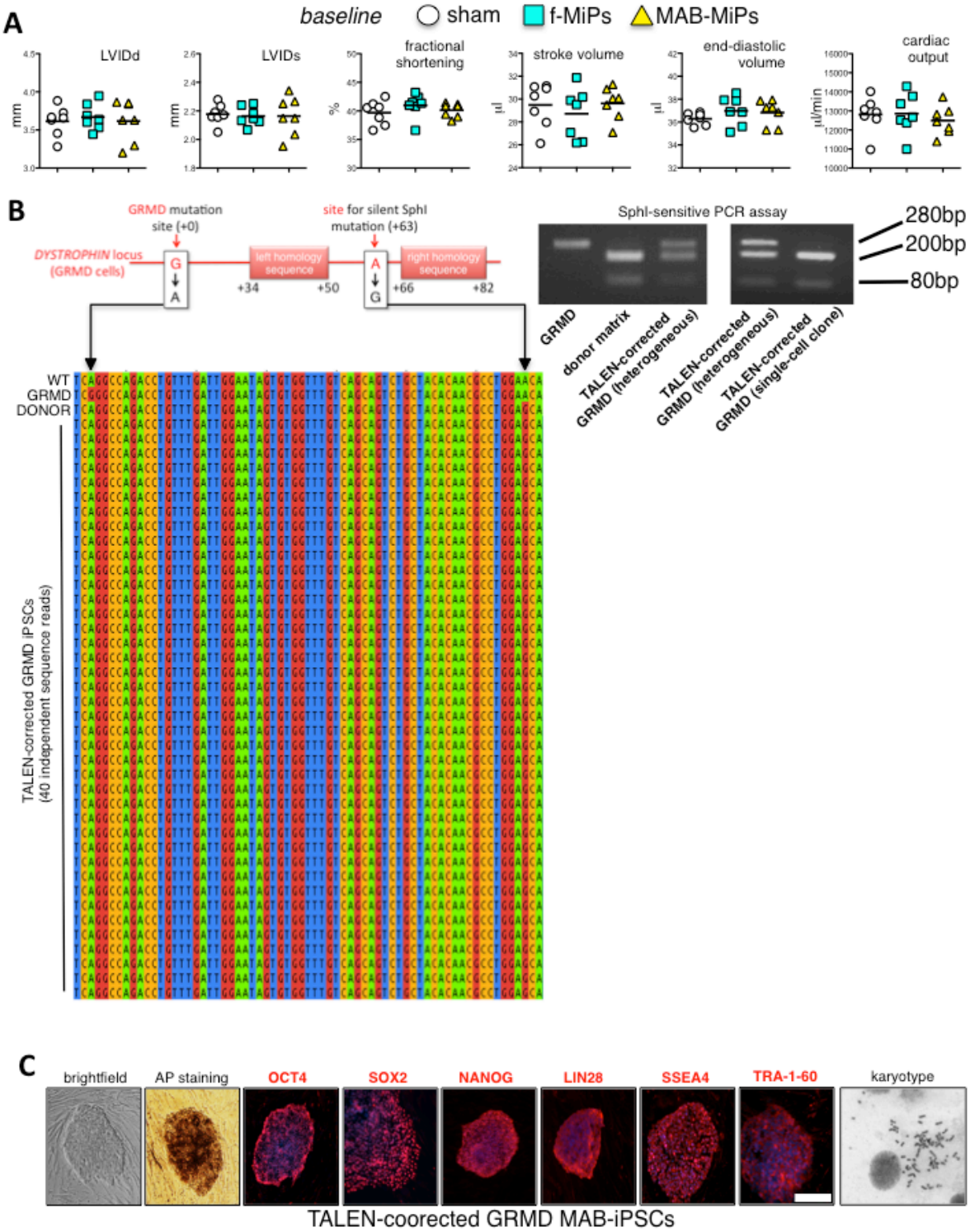

**Supplemental Figure 10. TALEN-based GRMD correction in canine MAB-iPSCs.** (**A**) 3D echocardiography analyses at baseline, i.e. prior to CAL and ctx injections, showed no significant differences among randomly-distributed mice cohorts; n=7mice/group, Kruskal-Wallis and Mann-Whitney tests. (**B**) Scheme of the TALEN vector design for the canine *DYSTROPHIN* locus, showing the sites of mutation correction and silent mutation integration, and the homology sequences recognized by the TALENs. (right panels) SphI assay on the specific amplicon encompassing the two homology sequences yielded two bands in the donor matrix (200bp and 80bp) and one undigested band (280bp) in the non-corrected cells. After electroporation and expansion, three bands, as expected, characterized the heterogeneous iPSC pool. After single cell-cloning, corrected GRMD iPSCs showed two bands, similarly to the donor matrix. (lower panels) Sequencing-based confirmation of the correction was performed by means of 40 independent clonal sequencing assays from the corrected GRMD iPSCs, showing homogeneous levels of mutation correction, SphI site integration, and reading frame maintenance (depicted is a ClustalW2 alignment of the sequences). (**C**) Corrected GRMD iPSCs maintained the characteristic features of morphology, pluripotency marker expression and euploidy.

## Supplemental Figure 11

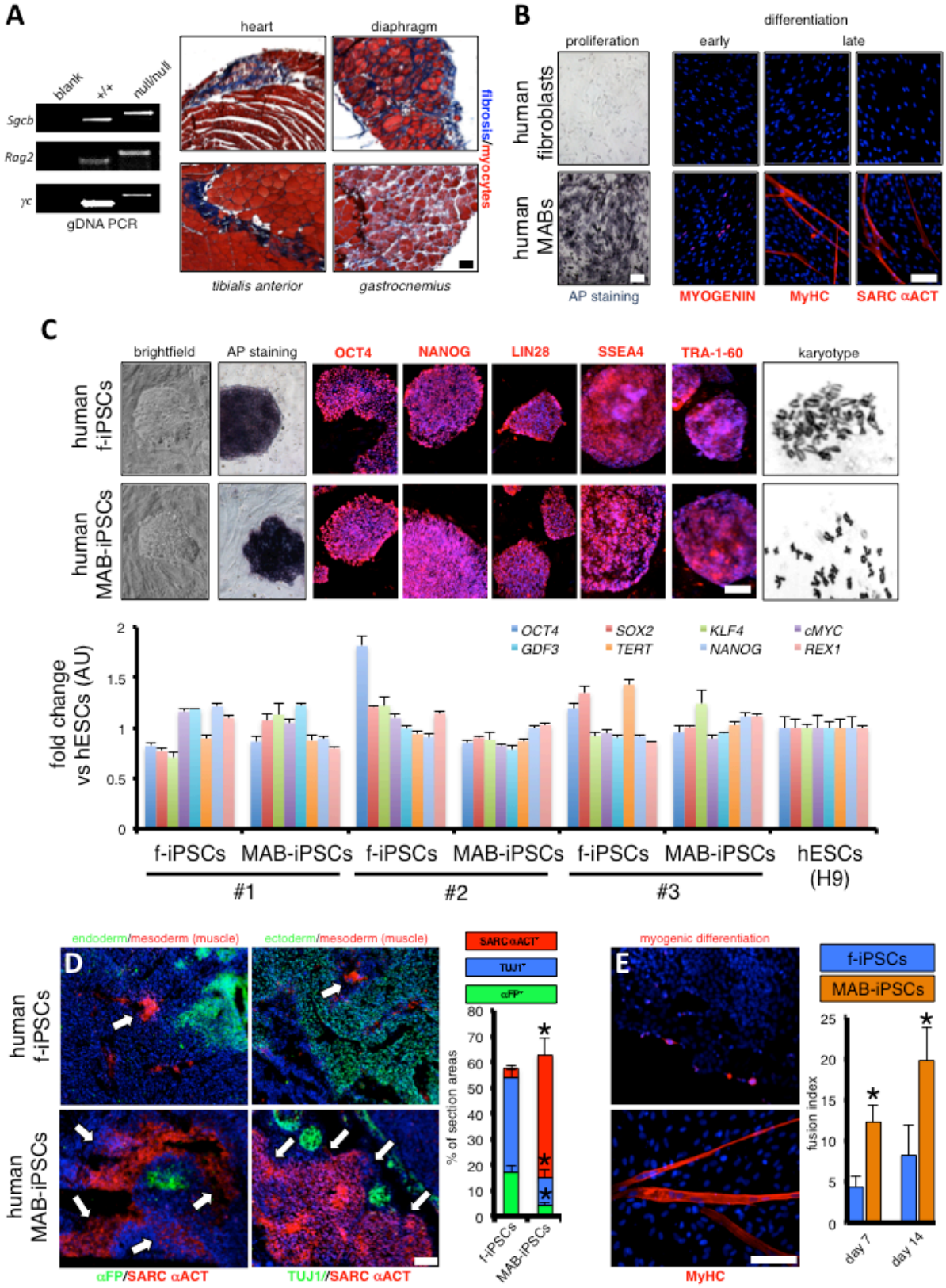

**Supplemental Figure 11. Characterization of dystrophic immunodeficient mice and of isogenic human iPSCs.** (**A**) *Sgcb-null/Rag2-null/γc-null* presented homozygous mutated alleles on all three loci and showed fibrosis, necrosis and dystrophic pathological features in cardiac and skeletal muscles at 3 months of age. (**B**) Isogenic human cells were differentiated through AP expression and myogenic markers of early and late myogenic differentiation during differentiation in serum starvation; n=3donors/cell type. (**C**) Isogenic human f- and MAB-iPSCs shared comparable features of hESC-like morphology and homogenous expression of pluripotency marker expression. Also, f- and MAB-iPSC clones from three independent reprogramming events appeared euploid and expressed pluripotency markers at comparable levels to hESCs (H9) grown in the same conditions. AU, arbitrary units; error bars, standard deviation; n=3donors/iPSC type. (**D**) Quantification of immunofluorescence staining fields (representative pictures are shown on the left) of teratomas obtained from human isogenic f- and MAB-iPSCs showed a significant increase in the immature muscle patches (SARC $\alpha ACT^+$) and decrease in endodermal glands and neuroectoderm formations ($\alpha FP^+$ and $TUJ^+$ respectively). *, $P<0.05$; n=4 teratomas/iPSC type; Mann-Whitney U test. (**E**) After over-expression pulse of *PAX7/MEF2C* by means of transient transfection, hMAB-iPSCs exhibited a significantly higher capacity of myogenic differentiation when compared to isogenic f-iPSCs, as shown by fusion index quantification at day 7 and 14 post-transfection. *, $P<0.05$; n=6/iPSC type; unpaired t-test. Scale bars, approximately 100μm.

**Supplemental Videos (1-4) –** Brightfield and fluorescence videos of $GFP^+$ isogenic murine f- (Suppl Videos 1-2) and MAB-MiPs (Suppl Videos 3-4) in co-culture with primary cultures of neonatal rat cardiomyocytes. Magnification, 20X.

**List of primers**

*mm*, *Mus musculus*. *cf* , *Canis familiaris*. *hs* , *Homo sapiens*. Fw, forward primer. Rev, reverse primer. All primer sequences are indicated in 5'-3' orientation.

**qPCR primers:**
*mmKlf4* Fw, AACTACCCTCCTTTCCTGCCAGA
*mmKlf4* Rev, ATAGTCACAAGTGTGGGTGGCTGT
*mmSox2* Fw, CACATGAAGGAGCACCCGGATTAT
*mmSox2* Rev, TCCGGGAAGCGTGTACTTATCCTT
*mmOct4* Fw, TGGAGGAAGCCGACAACAATGAGA
*mmOct4* Rev, TGGCGATGTGAGTGATCTGCTGTA
*mmcMyc* Fw, TAGTGTGTCTGTTCCAGCTACTGC
*mmcMyc* Rev, AACGTCTCTTCTCTACGGTGACCA
*mmRex1* Fw, GGCCAGTCCAGAATACCAGA
*mmRex1* Rev, GAACTCGCTTCCAGAACCTG
*mmLin28* Fw, CAGAAGCGAAGATCCAAAGG
*mmLin28* Rev, CAGGCTTTCCCTGAGAACTG
*mmGdf3* Fw, ACCTTTCCAAGATGGCTCCT
*mmGdf3* Rev, CCTGAACCACAGACAGAGCA
*mmDax1* Fw, TCCAGGCCATCAAGAGTTTC
*mmDax1* Rev, ATCTGCTGGGTTCTCCACTG
*mmNanog* Fw, ACAAGGGTCTGCTACTGAGATGCT
*mmNanog* Rev, AGAACACAGTCCGCATCTTCTGCT
*mmRunx1* Fw, AACAAGACCCTGCCCATCGCTTT
*mmRunx1* Rev, AACCTGAGGTCGTTGAATCTCGCT
*mmBrach* Fw, TGTGACCAAGAACGGCAG
*mmBrach* Rev, TCCCCGTTCACATATTTCCAG
*mmMeox1* Fw, AGGATTGCATGGTACTTGGG
*mmMeox1* Rev, CTCTCCTTCCGGGCTTTG
*mmMixl1* Fw, GTACCCAGACATCCACTTGC
*mmMixl1* Rev, TGAGGATAAGGGCTGAAATGAC
*mmGata4* Fw, TTTCTGGGAAACTGGAGCTG
*mmGata4* Rev, AGTCCTTGCTTTCTGCCTG
*mmFlk1* Fw, CTGTCGCTCTGTGGTTCTG
*mmFlk1* Rev, CTGTCCCCTGCAAGTAATCTG
*mmDesm* Fw, GAGCGTGACAACCTGATAGAC
*mmDesm* Rev, GTCAATACGAGCTAGAGTGGC
*mmPdgfb* Fw, TCCTCTCTGCTGCTACCTG
*mmPdgfb* Rev, CAGCCCCATCTTCATCTACG
*mmTbx5* Fw, CTCCGGCTTTCCTGCTAAG
*mmTbx5* Rev, CCAAAGCCCTCATCTGTATCG
*mmPax3* Fw, GGCAGAATTACCCACGCAG
*mmPax3* Rev, TCTTGTGGCGGATATGGTTG
*mmPax7* Fw, CAGAACTACCCGCGCAC
*mmPax7* Rev, ACTATCTTGTGACGGATGTGG

*mmNkx25* Fw, AAGTGCTCTCCTGCTTTCC
*mmNkx25* Rev, CGTCTCGGCTTTGTCCAG
*cfBRACHYURY* Fw, ACCGCTGGAAGTACGTGAAC
*cfBRACHYURY* Rev, TGAGCTTGTTGGTGAGCTTG
*cfNKX25* Fw, CCACCAACAACAACTTCGTG
*cfNKX25* Rev, CGGGAGTGAATGTGAAATCC
*cfFLK1* Fw, GATCGGTGAGAAATCCCTGA
*cfFLK1* Rev, CCTGGAAGTCATCCACGTTT
*cfTBX5* Fw, GCACAAATACCAGCCCAGAT
*cfTBX5* Rev, GGGAACCACGGGATATTCTT
*cfGATA4* Fw, AAGCTCCATGGTGTTCCAAG
*cfGATA4* Rev, GCATCTCTTCACTGCTGCTG
*cfDESMIN* Fw, ATTCCCTGATGAGGCAGATG
*cfDESMIN* Rev, AGGGCCATCTTGACATTGAG
*cfPAX7* Fw, AAGAAAGCCAAGCACAGCAT
*cfPAX7* Rev, AAGGCCTTCTCCAGCTCTTC
*cfPAX3* Fw, CCGAGTCCAGGTTTGGTTTA
*cfPAX3* Rev, TGGGCTGGTAAGATGTCTCC
*cfMEOX1* Fw, CATCCAGACGGAAAAAGGAG
*cfMEOX1* Rev, TCCACTTCATCCTTCGGTTC
*cfDYS* Fw, TTTCTGGCATATTAAAGATAGGACTTC
*cfDYS* Rev, GACCAAGAAATTTCAAAGGTCTCTA
*hsOCT4* Fw, CGAGCAATTTGCCAAGCTCCTGAA
*hsOCT4* Rev, GCCGCAGCTTACACATGTTCTTGA
*hsSOX2* Fw, CACATGAAGGAGCACCCGGATTAT
*hsSOX2* Rev, GTTCATGTGCGCGTAACTGTCCAT
*hsKLF4* Fw, AATTACCCATCCTTCCTGCCCGAT
*hsKLF4* Rev, TAATCACAAGTGTGGGTGGCGGT
*hsCMYC* Fw, TCCTCGGATTCTCTGCTCTCCT
*hsCMYC* Rev, AGAAGGTGATCCAGACTCTGACCT
*hsNANOG* Fw, TGGCCGAAGAATAGCAATGGTGTG
*hsNANOG* Rev, TTCCAGGTCTGGTTGCTCCACATT
*hsTERT* Fw, GAACATGCGTCGCAAACTCTTTGG
*hsTERT* Rev, CAGCACACATGCGTGAAACCTGTA
*hsREX1* Fw, TGGAGGAATACCTGGCATTGACCT
*hsREX1* Rev, AGCGATTGCGCTCAGACTGTCATA
*hsGDF3* Fw, ACACCTGTGCCAGACTAAGATGCT
*hsGDF3* Rev, TGACGGTGGCAGAGGTTCTTACAA
*mm/cfPGK* Fw, , CAAAATGTCGCTTTCCAACAAG
*mm/cfPGK* Rev, , AACGTTGAAGTCCACCCTCATC
*hsPGK* Fw, TGCCTGTTGACTTTGTCACTGCTG
*hsPGK* Rev, AGCCTCAGCATACTTCTTGCTGCT.

**Bisulphite sequencing primers:**

*Brach* Fw, TTTTATTGAATTATTTTTTGTTTTTTGTTA
*Brach* Rev, CCCAAATATAACAACTTTAAAACAC
*Meox1* Fw, TGAATTTGGGAGGTTTTTTTATAAA
*Meox1* Rev, CCTCTAAATCTAACCCCATCTAACC
*Mixl1* Fw, TGATTTTTTAGTATTTTTATTGGAA
*Mixl1* Rev, AAAAACAACTACTCCCAACCATAC
*Gata4* Fw, TTATTTGGTAAGAATTTTGTGTAGTT
*Gata4* Rev, ACCTCAATTTTCTCTCCTCTAAAAC
*Flk1* Fw, AAAGAGTGGGTTTTTTATTTATAGAGG
*Flk1* Rev, TCTTTCTACCCTAAATCCTCAAAAC
*Desmin* Fw, TTAGGAGGGTTATAAATAGTGTAGATAGTT
*Desmin* Rev, TAAACTCTTACAACTCCACCTTCTC
*Tbx5* Fw, TTTTTGGGGGTGTAAGAGTAGAGTA
*Tbx5* Rev, CAAAATACAAAACAAAACTAAAATCC
*Pax3* Fw, TTTTAGTTGGGGTTATTGGTAAAG
*Pax3* Rev, CACTAACTCTTACCACCCAAACTAC
*Pax7* Fw, TAAGGAAGTTTAAATAAATAAATATTTTAA
*Pax7* Rev, AACTAACCCCCTTTCCTACTCATAA
*Oct4* Fw, GGTTTTTTAGAGGATGGTTGAGTG
*Oct4* Rev, TCCAACCCTACTAACCCATCACC
*Nanog* Fw, GATTTTGTAGGTGGGATTAATTGTGAATTT
*Nanog* Rev, ACCAAAAAAACCCACACTCATATCAATATA.

**ChIP-qPCR primers:**

*Brach* Fw, CGAGAGGCAATAAACCAACTG
*Brach* Rev, TGGACTTTGACGGTGGATG
*Meox1* Fw, TGGAGAACACAAGACGCTG
*Meox1* Rev, AGTTGAAGGTTAGGAAGTGGC
*Mixl1* Fw, AAGACGAGCTCCAGCAAC
*Mixl1* Rev, CCAAACCGCGACTCCAG
*Gata4* Fw, CAGTGCAAAAGCAACCCAG
*Gata4* Rev, ATTTTCCTGAGATCCCCACG
*Flk1* Fw, GAAGTCACAGAGGCGGTATG
*Flk1* Rev, TGAAAGCCCAGACTGTGTC
*Desm* Fw, AGGGCTACAAATAGTGCAGAC
*Desm* Rev, TGGCTGGACGAGTAGGC
*Tbx5* Fw, CTGTTCCTCTAAGCCGTTCTG
*Tbx5* Rev, ACCACTAGAGCCTCCCAG
*Pax3* Fw, AGACACGCGCTGATTGG
*Pax3* Rev, GCCTCTCCTAGTTTCAACCTG
*Pax7* Fw, CTCTCAGCGCCTCTTTCTG
*Pax7* Rev, CTCGCTTTTCCTCTTGTGTTC
*Oct4* Fw, ACTGGTTTGTGAGGTGTCC
*Oct4* Rev, CTATCTGCCTGTGTCTTCCAG

*Nanog* Fw,  ACCTACCCTTTAAATCTATCGCC
*Nanog* Rev, TCCCACAGAAAGAGCAAGAC.